

Supporting Information

Recognition and location of motile microorganisms by shape- matching photoluminescence micro-patterns

*Meng Su,^a Zhandong Huang,^a Jing Liu,^b Yifan Li,^{a,d} Qi Pan,^{a,d} Zeying Zhang,^{a,d}
Zheng Li,^a Zheren Cai,^{a,d} Bingda Chen,^{a,d} Shuoran Chen,^c Fengyu Li,^{*a} and
Yanlin Song^{*a,d}*

^a Key Laboratory of Green Printing, CAS Research/Education Center for Excellence in Molecular Sciences, Institute of Chemistry, Chinese Academy of Sciences, Beijing 100190, P. R. China.

^b Institute of Laser and Intelligent Manufacturing Technology, South-Central University for Nationalities, Wuhan 430074, P. R. China

^c Research Center for Green Printing Nanophotonic Materials, Suzhou University of Science and Technology, Suzhou, 215009, P. R. China.

^d University of Chinese Academy of Sciences, Beijing 100049, P. R. China

*Corresponding author. Email: ylsong@iccas.ac.cn (Y.S.), forrest@iccas.ac.cn (F. L.)

Captions for Movie S1-4:

Movie S1. Micro-printing process recorded by the optical microscope.

Movie S2. Phototaxis microorganism recognition via the shape-matching interaction.

Movie S3. Microorganisms steered under the illumination from the BPEA star.

Movie S4. Recognition of *Ten dunaliella salinas* ($14\pm 2\ \mu\text{m}$) in the photoluminescence locks.

Supplementary Materials:

Templates and functional molecule used for molecular patterning via micro-printing strategy	Figure S1	Characterization of pillar-patterned silicon template.
	Figure S2	Characterization of 9,10-bis(phenylethynyl) anthracence (BPEA).
Micro-printing process and droplet deformation	Figure S3	Micro-printing process.
Photoluminescence characterization	Figure S4	Photoluminescence characterization.
Biological recognition	Figure S5 Figure S6 Figure S7 Figure S8 Figure S9	Microscale microorganism modulation.

Templates and functional molecule used for molecular patterning via micro-printing strategy

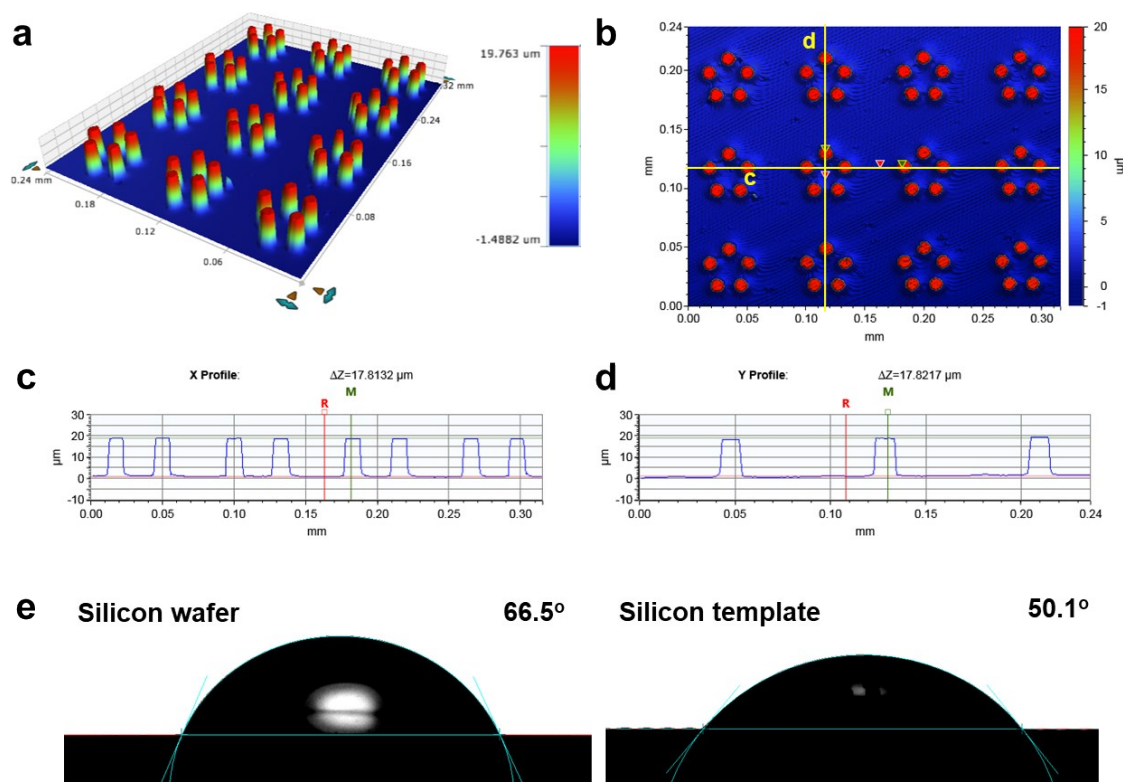


Figure S1. Characterization of pillar-patterned silicon template. a-b) 3D and 2D morphological figure of the pillar patterned template via the optical profiler. c-d) The height maps corresponding to the yellow lines in b. The height of the pillars is about 17 μm . e) Contact angles of silicon wafer and silicon template.

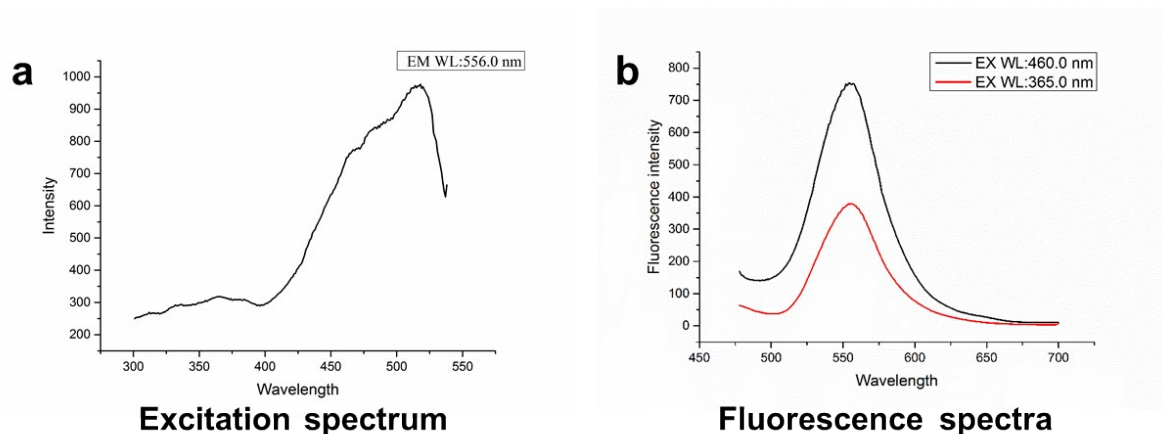


Figure S2. Characterization of 9,10-bis(phenylethynyl) anthracene (BPEA). a) Excitation spectrum of the BPEA. b) Fluorescence spectra of the BPEA with the excitation wavelength (460 nm and 365 nm).

Micro-printing process and droplet deformation

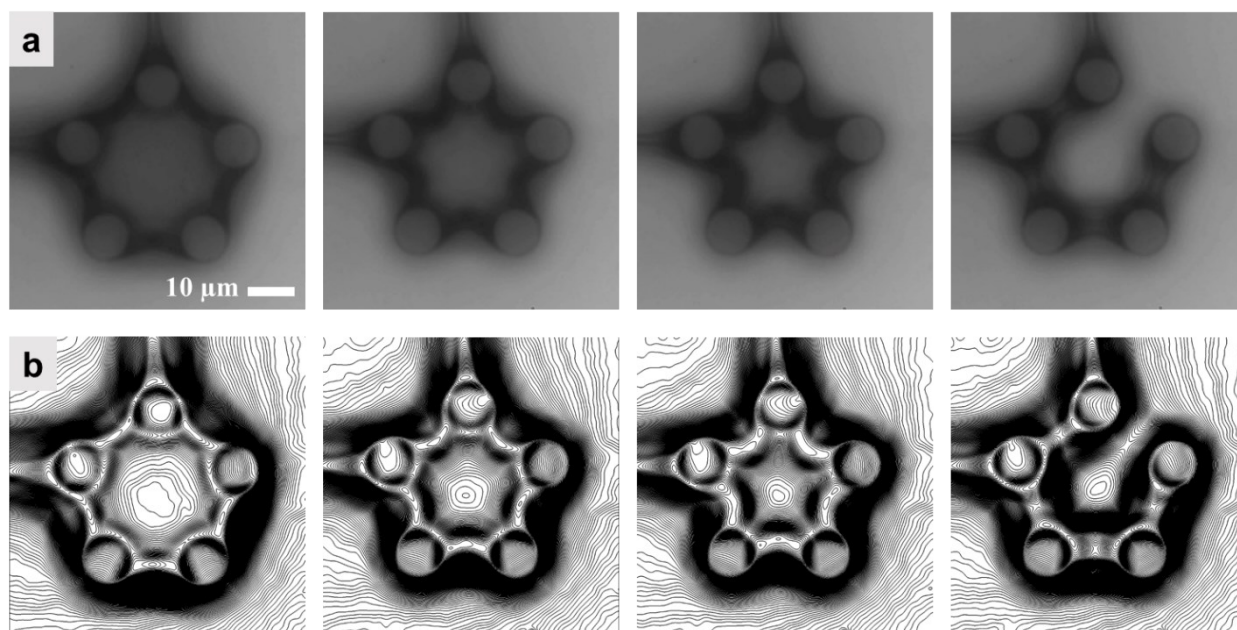


Figure S3. Micro-printing process. a) The micro-printing process was recorded by the dynamic video through optical microscope, which shows multiple droplet shapes with the evaporation of the solvent. b) The contracting process of the gas-liquid-solid three-phase contact line corresponds to the recorded process after image processing with ImageJ.

Photoluminescence characterization

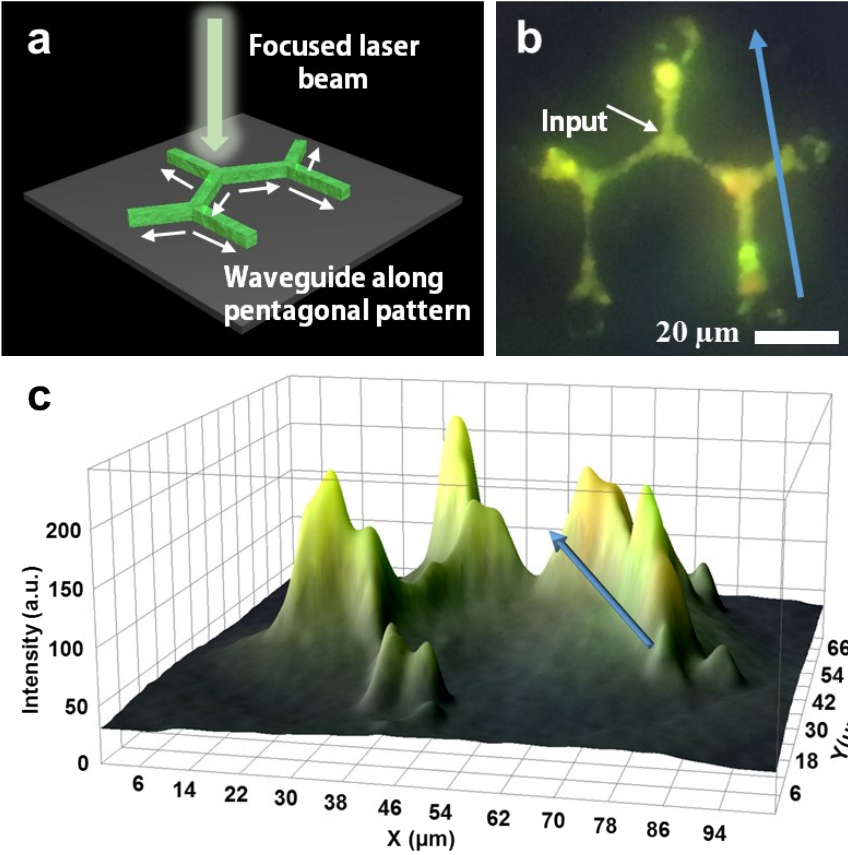


Figure S4. Photoluminescence characterization. a) Schematic illustration of photoluminescence along the BPEA micro-pattern after irradiated by the laser. A laser beam was focused on the center of micro-pattern to investigate the optical propagation. b) Photoluminescence image under a focused 407 nm laser beam excitation. The excitation position is indicated by the white arrow. c) 3D representation of the photoluminescence intensity in (b), the blue arrow corresponding to the one in (b). It shows area-covering photoluminescence even at the narrow junction.

Biological recognition

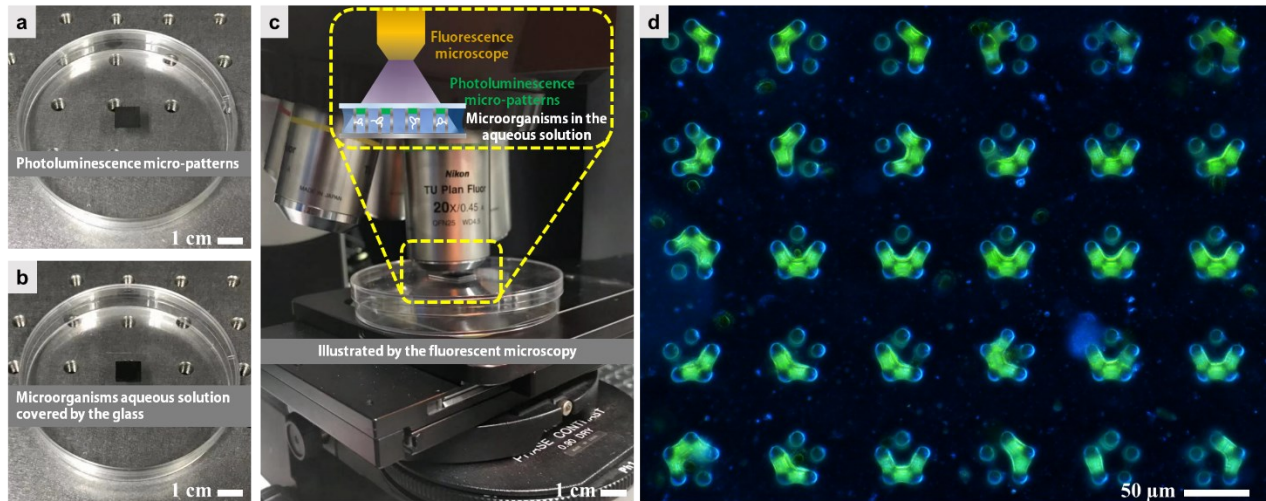


Figure S5. Equipment illustration for the shape-matching recognition of phototaxis microorganisms. a) Photograph of the photoluminescence locks on the silicon template. b) One drop (about 50 μL) of microorganisms aqueous solution was confined between the template and the cover glass. c) The photoluminescence locks are excited by the fluorescent microscopy. The shape-matching recognition of microorganisms are conducted while the ambient light is off. d) Microscopy image captured instantly after the microorganisms solution being dropped on the micro-patterns to show their initial positions.

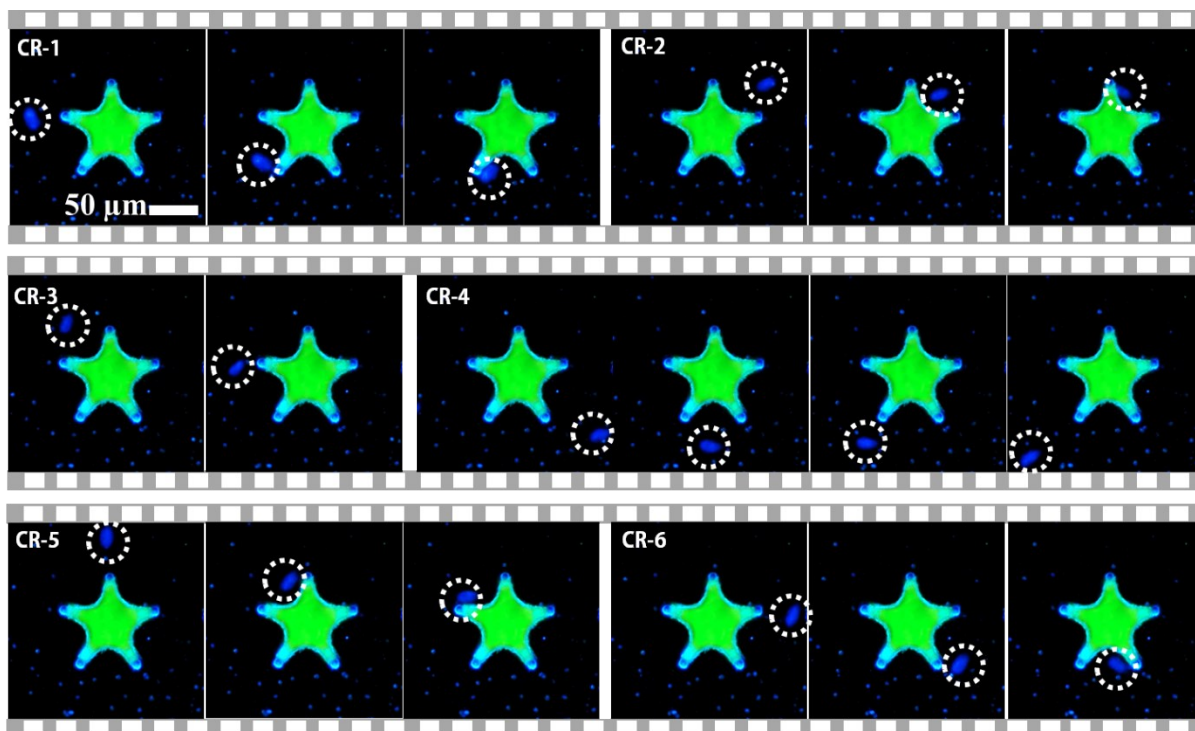


Figure S6. Sequential images of six CRs (CR-1, 2, 3, 4, 5 and 6) in the suspension with illumination from the BPEA star. It shows that all the microorganisms can be “steered” by using positive phototaxis under the illumination of the micro-pattern. A dashed circle has been added to each frame to indicate the position of the microorganism.

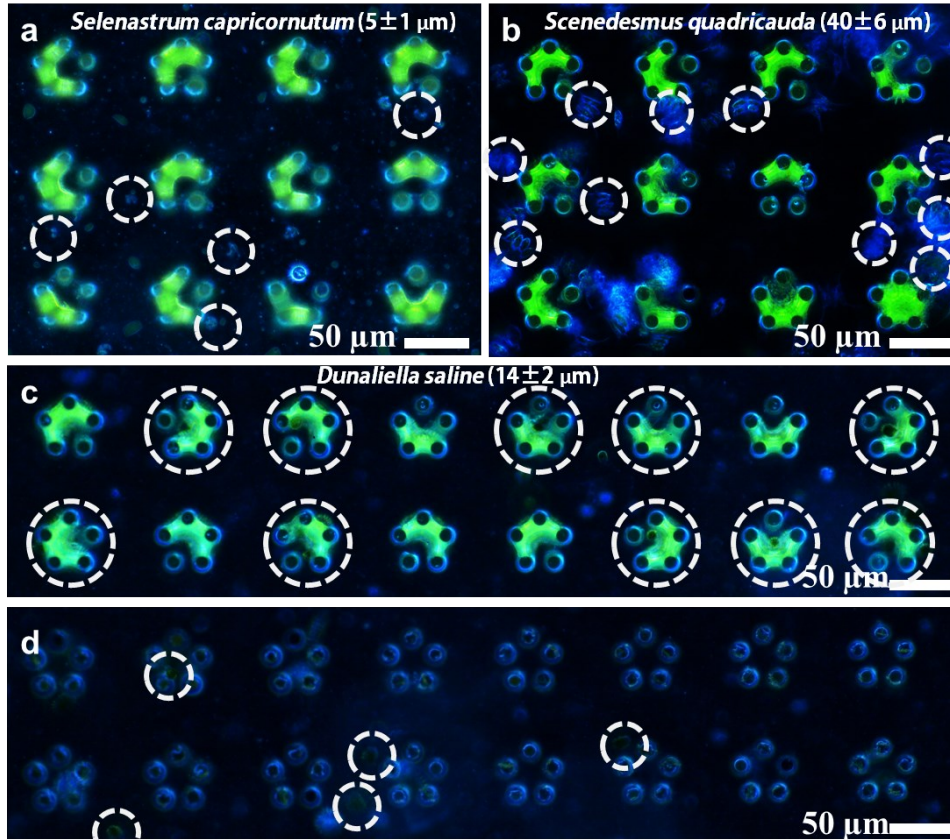


Figure S7. Mechanism illustration of shape-matching photoluminescence locks for localizing phototaxis microorganisms. a) *Selenastrum capricornutum* ($5 \pm 1 \mu\text{m}$) swim freely in and out of the locks without the shape-matching recognition. b) *Scenedesmus quadricauda* ($40 \pm 6 \mu\text{m}$) is too big to swim into the PL locks. c) Ten *dunaliella salina* ($14 \pm 2 \mu\text{m}$) are localized in the PL locks. d) *Dunaliella salina* cannot be localized in the scheduled position without the PL locks.

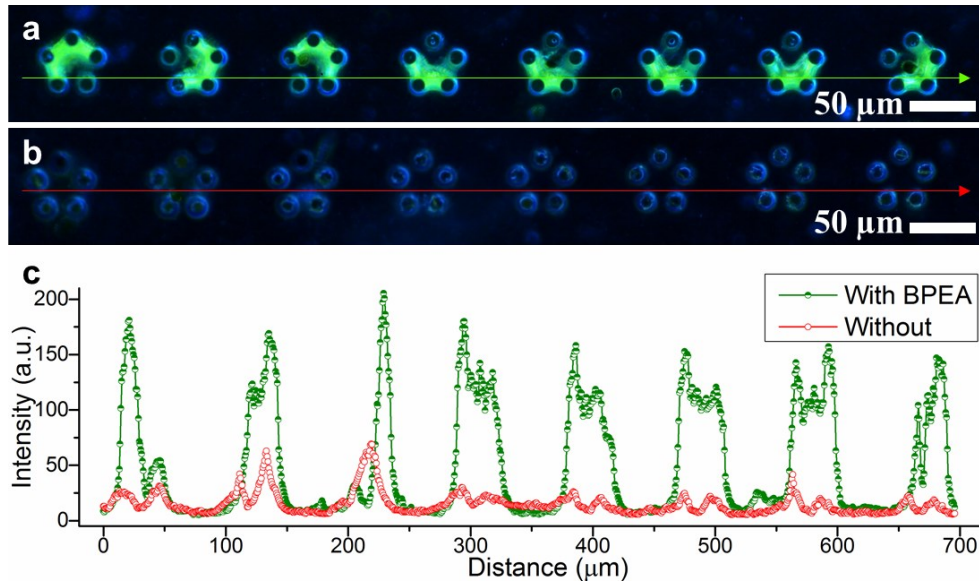


Figure S8. The contrast analysis of the light intensity with or without BPEA patterns. a-b) The photoluminescence images with or without BPEA patterns. c) The contrast analysis of the light intensity, indicating as the green and red arrows.

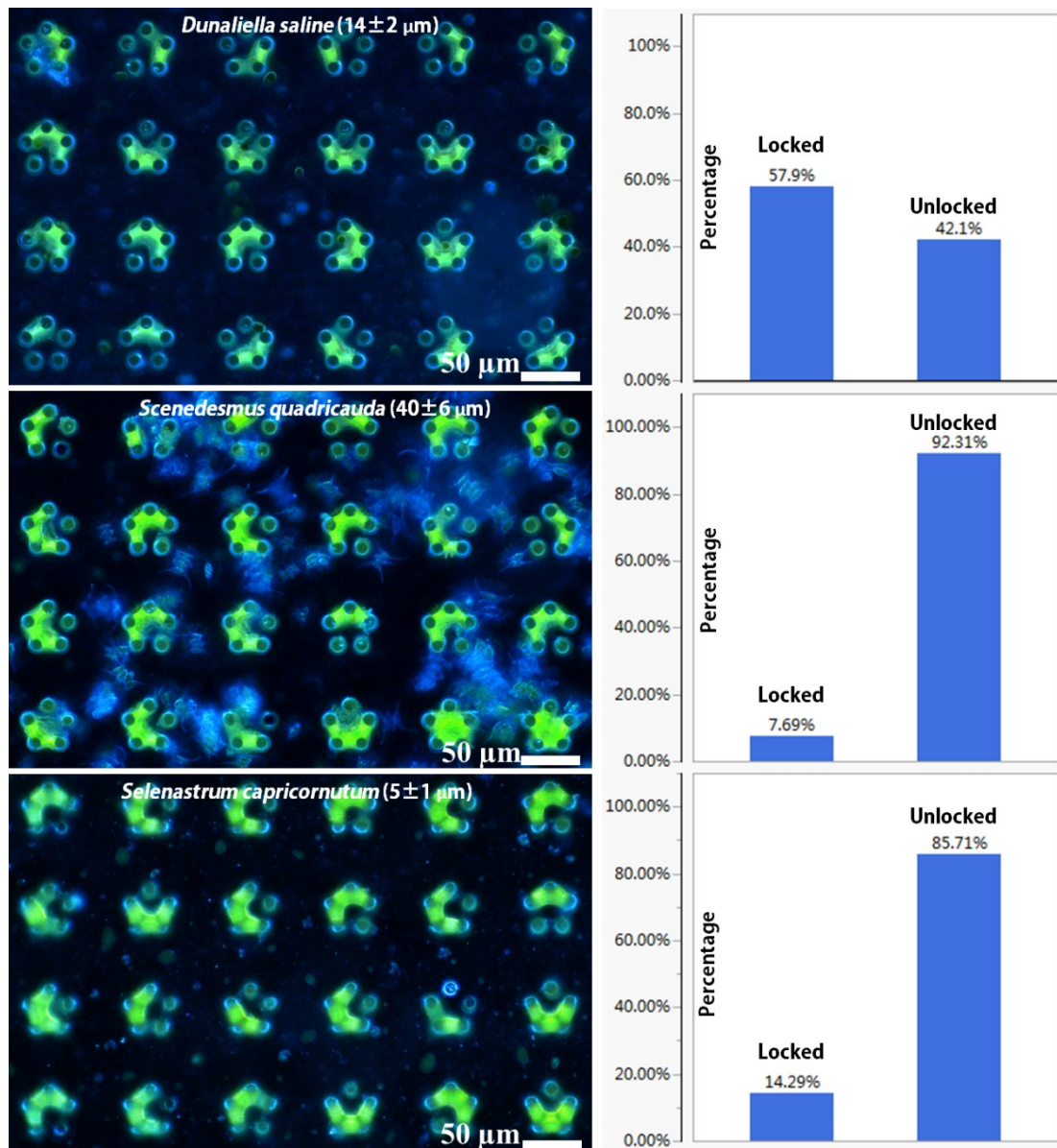


Figure S9. The numerical analysis of the size-selectivity of the BPEA patterns for different phototaxis microorganisms.